

Nuclear energy density functional and the nuclear α decay

Yeunhwan Lim^{1,*} and Yongseok Oh^{2,3,†}

¹*Cyclotron Institute and Department of Physics and Astronomy,
Texas A&M University, College Station, Texas 77843, USA*

²*Department of Physics, Kyungpook National University, Daegu 41566, Korea*

³*Asia Pacific Center for Theoretical Physics, Pohang, Gyeongbuk 37673, Korea*

The nuclear α decay of heavy nuclei is investigated based on the nuclear energy density functional, which leads to the α potential inside the parent nucleus in terms of the proton and neutron density profiles of the daughter nucleus. We use the Skyrme force model, Gogny force model, and relativistic mean field model to get the nucleon density profiles inside heavy nuclei. Once the nucleon density profiles are determined, the parameters of the nuclear α potential are fitted to the observed α decay half-lives of heavy nuclei. This approach is then applied to predict unknown α decay half-lives of heavy nuclei. To estimate the Q values of unobserved α decays, we make use of the liquid droplet model.

PACS numbers: 23.60.+e, 21.30.-x, 21.65.Ef, 27.90.+b

I. INTRODUCTION

The synthesis of unknown heavy nuclei has been spotlighted for last decades with the development of new facilities for rare isotope accelerators [1–3]. In particular, the structure of neutron-rich heavy nuclei is expected to shed light on our understanding of nuclear structure in isospin asymmetric nuclear matter and it will give insight on the structure of neutron stars and the process of nuclear synthesis during the evolution of stars [4]. Therefore, it can be a test ground for various issues of nuclear physics such as nuclear density functional, strong nuclear interactions, various decay processes, r-p process, etc, which makes it one of the most exciting topics in low energy nuclear physics [5]. The formation of such heavy nuclei is identified through their decay processes such as the α decay, β decay, and spontaneous fission [6]. The competition between these decay processes is reflected in branching ratios, and, in fact, the heavy nuclei with the atomic number $Z > 105$ were found to rarely survive for a few minutes [7, 8].

The study on the nuclear α decay process has a very long history, as it is one of the major decay processes of nuclei [6, 9]. In particular, the formation of a new heavy nuclide would be mostly identified through its α decay chains [10–12]. Modern approaches for theoretical understanding of the nuclear α decay are based on effective nuclear interactions such as the square well potential model [13, 14], cosh potential model [15], unified fission model [16], double-folding model [17–19], and so on.

The most important factor in the α decay process of heavy nuclei is the accurate information on the Q value for the decay process, which reflects the structure of heavy nuclei through binding energy. The importance of the Q value in the α decay lifetime can easily be found

in the Geiger-Nuttall law [20] and its improved version of Viola and Seaborg [6].¹

The next most sensitive factor in the determination of the α decay width is the nucleon distribution inside the daughter nucleus, which determines the α potential. Since the α -decay is basically a quantum tunneling effect, the exact positions of the classical turning points and the profile of the barrier, i.e., its height and width, are essential parts for the estimation of the α decay lifetime. Therefore, the information on the nuclear potential felt by the α cluster inside the parent nucleus is important to estimate the α decay width. Furthermore, the Coulomb potential is responsible for the repulsive potential barrier together with the angular momentum barrier, so the potential shape due to the proton distribution in the daughter nucleus has a nontrivial role in the α decay process. The purpose of the present work is to go beyond a simple model approach for the α potential by developing a more realistic α potential based on nucleon density profiles for estimating α decay half-lives.

In the present work, we calculate the α decay half-lives of heavy nuclei within the Wentzel-Kramers-Brillouin (WKB) approximation by calculating the nuclear potential felt by the α cluster using phenomenological nuclear force models. The nuclear potential form for the α cluster is obtained from the Skyrme-type interaction as prescribed in Ref. [21], which requires the proton and neutron distribution functions as inputs. We then use the Skyrme SLy4 model [22] and Gogny D1S model [23] as non-relativistic models and the relativistic mean-field DD-ME2 model [24] as well. For the Q values of the α decay processes, we use the experimental data whenever available, and, if not, we make use of the liquid droplet model (LDM) elucidated in Ref. [25].

¹ For example, in the case of the alpha decay of $^{212}\text{Po} \rightarrow ^{208}\text{Pb} + \alpha$, a difference of 0.1 MeV in the Q value of the reaction, where $Q_{\text{expt.}} \approx 8.95$ MeV, results in about a factor of 1.7 difference in the calculated half-life of ^{212}Po .

* ylim@tamu.edu

† yohphy@knu.ac.kr

This paper is organized as follows. In Sec. II, we review the LDM to calculate the binding energy to be used when the experimental Q value is not known. The Coulomb diffusion and exchange terms are included as well as the pairing and shell corrections, which gives a better fitting to existing data. In the shell corrections, we use the last magic number as a free variable to minimize the root-mean-square deviation of total binding energy. We also check the Q values using the phenomenological formula as a function of isospin asymmetry I , with $I = (N - Z)/A$, as in Ref. [16]. Section III briefly explains nuclear models to find the density profiles of nucleons inside nuclei, and we construct the effective nuclear potential for the α cluster. The parameters of the effective potential for each model of nucleon density distribution are determined. Our results are presented in Sec. IV and compared to experimental data. The predictions on the unobserved α decays of heavy nuclei are given as well. We summarize and conclude in Sec. V.

II. NUCLEAR MODELS

The Q value plays an important role to determine the lifetime of the α decay as it determines the assaulting frequency of the α particle for a given potential well. It also sets the penetration width for quantum tunneling. In the estimation of α decay lifetimes, we use the empirical Q values, if available. However, for unobserved decay processes, we have to resort to model predictions on the binding energy. In this Section, we review the LDM that will be used in the present work.

A. Liquid Droplet Model

To estimate the unknown binding energies of heavy nuclei, we make use of the LDM with some modifications as prescribed in Refs. [25, 26]. In general, heavy nuclei are neutron-rich and the neutron skin is likely to exist on the surface. For example, the neutron skin thickness of ^{208}Pb was investigated with the electric dipole response [27], the parity radius experiment (PREX) [28, 29], and, more recently, through coherent π^0 photoproduction [30]. All numerical calculations using Skyrme-Hartree-Fock, Gogny, and relativistic mean field models show the out-layer of neutrons in the neutron-rich heavy nuclei. Thus, it is natural to include the neutron skin effects in LDM. The binding energy in the LDM for a nucleus of (Z, A) is given as [25]

$$E = f_B (A - N_s) + 4\pi R^2 \sigma(\mu_n) + \mu_n N_s + E_{\text{Coul}} + E_{\text{pair}} + E_{\text{shell}}, \quad (1)$$

where f_B is the binding energy per baryon of infinite nuclear matter, N_s is the number of neutrons in the neutron skin on the surface, R is the radius of the nucleus, $\sigma(\mu_n)$ is the surface tension as a function of neutron chemical

potential μ_n . E_{Coul} is the Coulomb energy, E_{pair} is the pairing energy, and E_{shell} includes the shell corrections.

In this model, f_B is a phenomenological energy function, which reads

$$f_B = -B + S_v(1 - 2x)^2 + \frac{K}{18}(1 - u)^2, \quad (2)$$

where B is the binding energy per nucleon, S_v is the nuclear symmetry energy, and K is the nuclear incompressibility of symmetric nuclear matter at nuclear saturation density ρ_0 . Here, x and u are defined as

$$x = \frac{Z}{A - N_s}, \quad u = \frac{\rho}{\rho_0}. \quad (3)$$

The surface tension is a function of x , and we find that the simple expansion of $\sigma(x) = \sigma_0 - \sigma_\delta(1 - 2x)^2$ is not a good approximation for highly neutron-rich nuclei. Therefore, we use the form suggested in Refs. [31, 32], which reads

$$\sigma(x) = \sigma_0 \frac{2 \cdot 2^\alpha + q}{x^{-\alpha} + q + (1 - x)^{-\alpha}}. \quad (4)$$

The parameters σ_0 , α , and q will be determined later.

The Coulomb energy contribution to the total mass is obtained from the classical Coulomb interaction, the Coulomb diffusion term, and the exchange term. It is then written as

$$E_{\text{Coul}} = \frac{3Z^2e^2}{5R} - \frac{\pi^2 Z^2 e^2 d^2}{2R^3} - \frac{3Z^{4/3}e^2}{4R} \left(\frac{3}{2\pi}\right)^{2/3}, \quad (5)$$

where d ($= 0.55$ fm) is the surface diffuseness parameter [25] and R is the average radius of the nucleus. The general expression for the pairing energy in LDM reads

$$E_{\text{pair}} = (-1)^N \frac{\Delta_N}{\sqrt{A}} + (-1)^Z \frac{\Delta_P}{\sqrt{A}}, \quad (6)$$

where the pairing energies for protons and neutrons are treated separately, since neutron-rich nuclei would have higher single particle energy of the last-filled neutron than the one for protons.

For the shell contribution to the total binding energy, we follow the prescription of Duflo and Zuker [33, 34], which writes the shell correction as

$$E_{\text{shell}} = a_1 S_2 + a_2 (S_2)^2 + a_3 S_3 + a_{np} S_{np}, \quad (7)$$

where a_1 , a_2 , a_3 , and a_{np} are parameters to be determined, and

$$\begin{aligned} S_2 &= \frac{n_v \bar{n}_v}{D_n} + \frac{p_v \bar{p}_v}{D_p}, \\ S_3 &= \frac{n_v \bar{n}_v (n_v - \bar{n}_v)}{D_n} + \frac{p_v \bar{p}_v (p_v - \bar{p}_v)}{D_p}, \\ S_{np} &= \frac{n_v \bar{n}_v p_v \bar{p}_v}{D_n D_p}. \end{aligned} \quad (8)$$

	Case I	Case II	Unit
B	16.125	16.370	MeV
ρ_0	0.155	0.155	fm^{-3}
σ_0	1.256	1.300	MeV fm^{-2}
α	4.0	3.7	
q	60.00	25.48	
S_v	31.818	32.471	MeV
K	250.00	226.389	MeV
Δ_n	5.458	6.232	MeV
Δ_p	5.807	11.760	MeV
a_1	1.265	-0.143	MeV
a_2	-8.601×10^{-3}	9.307×10^{-3}	MeV
a_3	-4.007×10^{-3}	2.216×10^{-3}	MeV
a_{np}	-9.663×10^{-2}	-4.231×10^{-2}	MeV
$M(8)$	184	168	
RMSD	1.144	0.218	MeV

TABLE I. The parameters of LDM. The values of case I are obtained by the least χ^2 fitting to the observed binding energies for 2336 nuclei. The parameters in case II are found by fitting to the experimental Q values for the nuclei with $Z \geq 100$, where we have totally 100 data points. $M(8)$ is the 8th magic number in each case. RMSD in the last row denotes the root-mean-square deviation. The RMSD in cases I is for binding energies, whereas that in case II is for Q values.

Here, n_v and p_v are the valence numbers of neutrons and protons, respectively, i.e., the minimal difference for neutron and proton numbers from the magic numbers, 2, 8, 20, 28, 50, 82, 126, and 184 (or 168). For example, for ^{56}Fe , we obtain $n_v = |30 - 28| = 2$ and $p_v = |26 - 28| = 2$. D_n (D_p) is the degeneracy number, i.e., the interval of the magic numbers adjacent to the neutron (proton) number. For instance, in the case of ^{56}Fe , the nearest two magic numbers for $N = 30$ are 28 and 50, which then leads to $D_{N=30} = 50 - 28 = 22$. Finally, \bar{n}_v and \bar{p}_v are the complementary valence numbers for neutrons and protons, respectively, and their explicit forms are

$$\bar{n}_v \equiv D_n - n_v, \quad \bar{p}_v \equiv D_p - p_v. \quad (9)$$

Again, for ^{56}Fe , we have $\bar{n}_v(30) = 22 - 2 = 20$.

In the present work, we will work with two parameter sets as given in Table I. The parameters of case I are obtained by fitting to the experimentally known binding energies of 2336 nuclei. Therefore, this corresponds to a global fitting. On the other hand, since we are considering α decays of neutron-rich heavy nuclei, it may be useful to focus on heavy nuclei for that purpose. Thus the second parameter set is found by using the measured Q values of heavy nuclei with $Z \geq 100$. We use 100 data points for finding the parameters set of case II. Note that $M(8)$ in Table I is the 8th magic number in the LDM parameterization with each parameter set.

Once the masses of nuclei are evaluated by Eq. (1), we can calculate the Q value for α decay through [35]

$$Q = \Delta M(Z, A) - \Delta M(Z - 2, A - 4) - \Delta M_\alpha$$

a	b	c	d	e	RMSD
0.90753	-97.84028	16.15924	-18.95722	-26.16600	0.255

TABLE II. The best fit parameters of Eq. (11). All parameters have a unit of MeV.

$$+ 10^{-6} k [Z^\beta - (Z - 2)^\beta], \quad (10)$$

where $\Delta M_\alpha = 2.4249$ MeV. The values for k and β are ($k = 8.7$ MeV, $\beta = 2.517$) for nuclei of $Z \geq 60$, and ($k = 13.6$ MeV, $\beta = 2.408$) for nuclei of $Z < 60$.

B. Local formula for Q_α

Considering heavy nuclei with $Z \geq 90$ and $N \geq 140$, Dong et al. [16, 36] developed a local mass formula for nuclei with large N and Z values. Using the Taylor expansion, it leads to the expression of the local Q value including shell effects as

$$Q = a \frac{Z}{A^{4/3}} (3A - Z) + b \left(\frac{N - Z}{A} \right)^2 + c \left[\frac{|N - 152|}{N} - \frac{|N - 154|}{N - 2} \right] + d \left[\frac{|Z - 110|}{Z} - \frac{|Z - 112|}{Z - 2} \right] + e, \quad (11)$$

where a , b , c , d , and e are parameters to be fitted. Note that the pairing effects are neglected since the semi-classical formula gives almost the same contribution to the total binding energy for both parent and daughter nuclei and it does not cause a change in the Q value. Since our goal is to compute the half-lives of super heavy nuclei through α decay processes, we obtain the parameters in Eq. (11) with the measured Q values for nuclei with $Z \geq 100$. The resulting parameters are shown in Table II.

Figure 1 shows the Q values obtained from the LDM with Eq. (10) and those from the local formula of Eq. (11). It is found that the case II and the local formula give more reliable results than case I on the measured Q values.

III. POTENTIAL FOR THE α CLUSTER

In the α cluster model, the nuclear α decay is described as a quantum tunneling effect. Once the energy, i.e., the Q value, of the reaction is determined, the next step is to find the potential for the α cluster inside the parent nucleus. In this Section, we discuss how we use phenomenological models for constructing the potential for the α cluster.

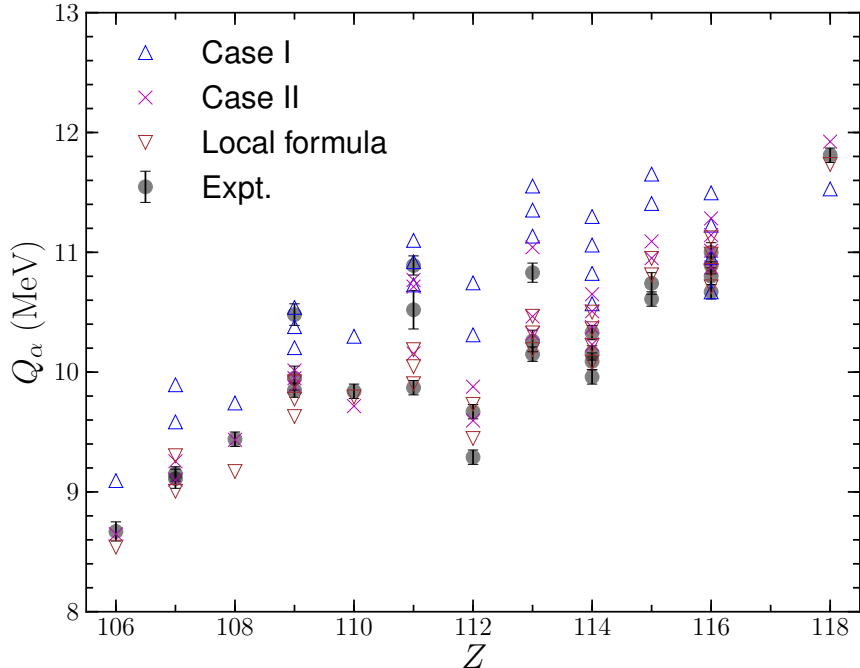


FIG. 1. Q values for α decays of nuclei between $Z = 106$ and $Z = 118$. The numerical values can be found in Table IV. A small horizontal offset is used for better visibility for a given value of Z .

A. Potential form

In the α cluster model, the α particle is already formed in the parent nucleus and it penetrates the potential barrier to cause the α decay process. Therefore, the estimation of lifetimes requires the information on the potential of the α cluster created by the core nucleus, i.e., the daughter nucleus after decay.

The α cluster potential can be decomposed as

$$V = V_N + V_C + V_L, \quad (12)$$

where V_N is the nuclear potential for the α cluster, V_C is the Coulomb potential provided by the protons of the core nucleus, and V_L is the centrifugal potential arising from the relative orbital angular momentum between the α particle and the core nucleus. In principle, the nuclear potential of the α particle would be computed if the interactions between nucleons inside a nucleus is completely known. However, it is certainly beyond the scope of the present work, and we invoke the Skyrme force model to get the form of V_N . Then, as described in Ref. [21], V_N takes the form of

$$V_N = \alpha\rho + \beta(\rho_n^{5/3} + \rho_p^{5/3}) + \gamma\rho^\epsilon(\rho^2 + 2\rho_n\rho_p) + \delta\frac{1}{r}\frac{d\rho}{dr} + \eta\frac{d^2\rho}{dr^2}, \quad (13)$$

where $\rho = \rho_n + \rho_p$ with ρ_n (ρ_p) being the density distribution of neutrons (protons). This model contains 6 parameters, namely, α , β , γ , δ , η , and ϵ . These parameters will be determined by fitting to the empirical data for

α decay half-lives of heavy nuclei and will be discussed in the next subsection. Furthermore, the nuclear potential in Eq. (13) is controlled by the density distribution of nucleons, which should be provided by microscopic models for nuclear structure.

Once the nucleon distribution is known, the Coulomb potential term V_C can be calculated through

$$V_C = 8\pi e^2 \left[\frac{1}{r} \int_0^r \rho_p(r') r'^2 dr' + \int_r^\infty \rho_p(r') r' dr' \right]. \quad (14)$$

The centrifugal potential V_L is written as

$$V_L = \frac{\hbar^2}{2m_\mu r^2} \left(\ell + \frac{1}{2} \right)^2, \quad (15)$$

where m_μ is the reduced mass, and the Langer modification factor [37] is adopted.

B. Nucleon density profiles

Since the α cluster potential of Eq. (13) requires the information on the density profile of the daughter nucleus, we rely on microscopic models for nuclear structure. In the present work, we consider the Skyrme SLy4 (zero-range) [22] and the Gogny D1S (finite-range) [23] models as non-relativistic approaches and the relativistic mean-field interaction DD-ME2 model of Ref. [24] as a relativistic approach.

The Skyrme force model is constructed based on nucleon-nucleon interactions having dependence on the

relative momentum and density, which reads

$$\begin{aligned}
v_{ij} = & t_0 (1 + x_0 P_\sigma) \delta(\mathbf{r}_i - \mathbf{r}_j) \\
& + \frac{t_1}{2} (1 + x_1 P_\sigma) \\
& \quad \times [\delta(\mathbf{r}_i - \mathbf{r}_j) \mathbf{k}^2 + \mathbf{k}'^2 \delta(\mathbf{r}_i - \mathbf{r}_j)] \\
& + t_2 (1 + x_2 P_\sigma) \mathbf{k}' \cdot \delta(\mathbf{r}_i - \mathbf{r}_j) \mathbf{k} \\
& + \frac{t_3}{6} (1 + x_3 P_\sigma) \rho^\alpha \delta(\mathbf{r}_i - \mathbf{r}_j) \\
& + i W_0 \mathbf{k}' \delta(\mathbf{r}_i - \mathbf{r}_j) \times \mathbf{k} \cdot (\boldsymbol{\sigma}_i + \boldsymbol{\sigma}_j), \quad (16)
\end{aligned}$$

where P_σ is the spin exchange operator, and $\boldsymbol{\sigma}_i$ are the Pauli spin matrices. Here, \mathbf{k} and \mathbf{k}' are the relative momenta of two nucleons before and after interaction, respectively, and W_0 is the strength of the spin-orbit coupling. There are many versions of the parameter set (t_i, x_i, W_0) and, in the present work, we use the SLy4 model compiled in Ref. [22].

Compared with the Skyrme force model, the Gogny force assumes finite-range nucleon-nucleon interactions and zero-range multi-body forces, which leads to [38]

$$\begin{aligned}
v_{12} = & \sum_{j=1,2} \exp \left\{ -\frac{(\mathbf{r}_1 - \mathbf{r}_2)^2}{\mu_j^2} \right\} \\
& \times (W_j + B_j P_\sigma - H_j P_\tau - M_j P_\sigma P_\tau) \\
& + t_0 (1 + x_0 P_\sigma) \rho^\alpha \left(\frac{\mathbf{r}_1 + \mathbf{r}_2}{2} \right) \delta(\mathbf{r}_1 - \mathbf{r}_2) \\
& + i W_{LS} \mathbf{k}' \delta(\mathbf{r}_1 - \mathbf{r}_2) \times \mathbf{k} \cdot (\boldsymbol{\sigma}_1 + \boldsymbol{\sigma}_2), \quad (17)
\end{aligned}$$

where P_τ is the isospin exchange operator. We use the parameter values known as the D1S model in Ref. [23].

For nucleon density distribution, we also use a relativistic mean-field model of Refs. [24, 39], which gives a satisfactory description for the properties of finite nuclei. In this model, the relativistic Lagrangian density is given by

$$\begin{aligned}
\mathcal{L} = & \bar{\psi} (i\partial - m) \psi + \frac{1}{2} \partial^\mu \sigma \partial_\mu \sigma - \frac{1}{2} m_\sigma \sigma^2 - g_\sigma \bar{\psi} \sigma \psi \\
& - \frac{1}{4} \Omega^{\mu\nu} \Omega_{\mu\nu} + \frac{1}{2} m_\omega^2 \omega^2 - g_\omega \bar{\psi} \gamma^\mu \omega_\mu \psi \\
& - \frac{1}{4} \vec{R}^{\mu\nu} \cdot \vec{R}_{\mu\nu} + \frac{1}{2} m_\rho^2 \vec{\rho}^2 - g_\rho \bar{\psi} \gamma^\mu \vec{\rho}_\mu \cdot \vec{\tau} \psi \\
& - \frac{1}{4} F^{\mu\nu} F_{\mu\nu} - e \bar{\psi} \gamma^\mu A_\mu \frac{(1 - \tau_3)}{2} \psi, \quad (18)
\end{aligned}$$

where $\Omega^{\mu\nu}$, $\vec{R}^{\mu\nu}$, and $F^{\mu\nu}$ are the field strength tensors of the ω vector meson field ω_μ , the isovector ρ vector meson field $\vec{\rho}_\mu$, and the photon field A_μ , respectively. Note that the coupling constants of mesons to the nucleon are density-dependent so as to reproduce the properties of nuclear matter and finite nuclei. In the present work, we adopt the parameter set given as the DD-ME2 model in Ref. [24].

Within the Skyrme and Gogny force models, we solve Schrödinger-like equations to obtain the density profile of a nucleus. On the other hand, in the relativistic mean

Parameter	SLy4	D1S	DD-ME2	Unit
α	-1484.58	-1499.04	-1524.24	MeV fm ³
β	1355.57	1248.80	1289.04	MeV fm ⁵
γ	1005.48	242.28	1137.21	MeV fm ^{6+ϵ}
δ	53.87	30.75	-41.84	MeV fm ⁵
η	-210.15	-178.12	-184.09	MeV fm ⁵
ϵ	1/6	1/3	1/6	

TABLE III. Parameters for α particle potential in Eq. (13).

field model, we solve the Dirac equation to get the density profile for a given nucleus. Once the density profile is known, one can find the α potential for each nucleus and the α decay lifetime can be computed. Since the α potential in Eq. (12) contains 6 parameters, we determine these parameters to the experimental data for the alpha decays of even-even nuclei ($\ell = 0$) as we have done in Ref. [21]. Table III shows the parameters for the nuclear α potential determined in this manner. The potential parameters for each model are found to have similar magnitudes except the case of γ , which is correlated to the value of ϵ . The γ term is related with the multi-body force and we choose $\epsilon = \frac{1}{3}$ in the Gogny D1S model reflecting the original ϵ value in the Gogny NN interaction.

IV. RESULTS

Equipped with the α potential obtained in the previous section, the α -decay half-lives of heavy nuclei can be estimated in the standard way by using the WKB approximation. The half-life of the nuclear α decay is related to the decay width Γ by

$$T_{1/2} = \frac{\hbar \ln 2}{\Gamma}, \quad (19)$$

where the decay width is given by

$$\Gamma = \mathcal{P} \mathcal{F} \frac{\hbar^2}{4m_\mu} \exp \left[-2 \int_{r_2}^{r_3} dr k(r) \right]. \quad (20)$$

Here, \mathcal{P} is the preformation factor which illustrates the probability of α particle in the parent nuclei, and \mathcal{F} is the assaulting frequency of the trapped α particle between two turning points r_1 and r_2 . In this calculation, we use $\mathcal{P} = 1$ and the explicit expression for \mathcal{F} can be found, for example, in Ref. [21]. The distance between r_2 and r_3 , i.e., $|r_2 - r_3|$, represents the penetration width of the barrier through which α particle passes. $k(r)$ corresponds to the wave number of the α particle inside the potential barrier,

$$k(r) = \sqrt{\frac{2m_\mu}{\hbar^2} |Q - V(r)|} \quad (21)$$

with m_μ being the reduced mass of the system.

TABLE IV. Observed α decay half-lives of heavy nuclei and the results of the present work. Unless specified, $\ell = 0$ is understood.

(Z, A)	Q_{α}^{Expt} (MeV)	$T_{1/2}^{\text{Expt}}$	$T_{1/2}^{\text{SLy4}}$ [ℓ]	$T_{1/2}^{\text{D1S}}$ [ℓ]	$T_{1/2}^{\text{DD-ME2}}$ [ℓ]	Reference
(118, 294)	11.81 ± 0.06	$0.89_{-0.31}^{+1.07}$ ms	$0.50_{-0.13}^{+0.18}$ ms	$0.61_{-0.16}^{+0.22}$ ms	$0.43_{-0.11}^{+0.15}$ ms	[40]
(116, 293)	10.67 ± 0.06	53_{-19}^{+62} ms	65_{-20}^{+28} ms	78_{-23}^{+33} ms	54_{-16}^{+24} ms	[41]
(116, 292)	10.80 ± 0.07	18_{-6}^{+16} ms	31_{-10}^{+16} ms	38_{-13}^{+19} ms	26_{-9}^{+13} ms	[41]
(116, 291)	10.89 ± 0.07	18_{-6}^{+22} ms	19_{-9}^{+9} ms	23_{-7}^{+11} ms	16_{-5}^{+8} ms	[40]
(116, 290)	11.00 ± 0.08	$7.1_{-1.7}^{+3.2}$ ms	$10.6_{-3.8}^{+6.1}$ ms	$12.5_{-4.5}^{+7.2}$ ms	$8.6_{-3.1}^{+5.0}$ ms	[40]
(115, 288)	10.61 ± 0.06	87_{-30}^{+105} ms	51_{-15}^{+21} ms	57_{-17}^{+25} ms	42_{-13}^{+19} ms	[42, 43]
(115, 287)	10.74 ± 0.09	32_{-14}^{+155} ms	25_{-10}^{+17} ms	28_{-12}^{+20} ms	21_{-9}^{+15} ms	[42, 43]
(114, 289)	9.96 ± 0.06	$2.7_{-0.7}^{+1.4}$ s	$1.3_{-0.4}^{+0.6}$ s	$1.5_{-0.5}^{+0.7}$ s	$1.0_{-0.3}^{+0.5}$ s	[41]
(114, 288)	10.09 ± 0.07	$0.8_{-0.18}^{+0.32}$ s	$0.56_{-0.20}^{+0.31}$ s	$0.65_{-0.23}^{+0.37}$ s	$0.46_{-0.16}^{+0.26}$ s	[41]
(114, 287)	10.16 ± 0.06	$0.48_{-0.09}^{+0.16}$ s	$0.37_{-0.12}^{+0.17}$ s	$0.42_{-0.13}^{+0.20}$ s	$0.31_{-0.10}^{+0.15}$ s	[40]
(114, 286)	10.33 ± 0.06	$0.13_{-0.02}^{+0.04}$ s	$0.14_{-0.05}^{+0.06}$ s	$0.15_{-0.05}^{+0.07}$ s	$0.12_{-0.04}^{+0.05}$ s	[40]
(113, 284)	10.15 ± 0.06	$0.48_{-0.17}^{+0.58}$ s	$0.20_{-0.06}^{+0.09}$ s	$0.23_{-0.07}^{+0.10}$ s	$0.28_{-0.09}^{+0.13}$ s [$\ell = 2$]	[42, 43]
(113, 283)	10.26 ± 0.09	100_{-45}^{+490} ms	106_{-45}^{+77} ms	120_{-51}^{+89} ms	94_{-40}^{+70} ms	[42, 43]
(113, 282)	10.83 ± 0.08	73_{-29}^{+134} ms	106_{-38}^{+62} ms [$\ell = 6$]	121_{-45}^{+73} ms [$\ell = 6$]	93_{-34}^{+55} ms [$\ell = 6$]	[44]
(112, 285)	9.29 ± 0.06	34_{-9}^{+17} s	27_{-10}^{+14} ms	30_{-10}^{+16} s	22_{-8}^{+13} s	[41]
(112, 283)	9.67 ± 0.06	$3.8_{-0.7}^{+1.2}$ s	$2.0_{-0.7}^{+1.0}$ s	$2.3_{-0.8}^{+1.2}$ s	$1.8_{-0.6}^{+0.9}$ s	[40]
(111, 280)	9.87 ± 0.06	$3.6_{-1.3}^{+4.3}$ s	$1.4_{-0.4}^{+0.7}$ s [$\ell = 4$]	$1.6_{-0.5}^{+0.8}$ s [$\ell = 4$]	$7.2_{-2.3}^{+3.4}$ s [$\ell = 6$]	[42, 43]
(111, 279)	10.52 ± 0.16	170_{-80}^{+810} ms	157_{-95}^{+251} ms [$\ell = 6$]	176_{-106}^{+276} ms [$\ell = 6$]	138_{-83}^{+219} ms [$\ell = 6$]	[42, 43]
(111, 278)	10.89 ± 0.08	$4.2_{-1.7}^{+7.5}$ ms	$3.5_{-1.3}^{+1.9}$ ms [$\ell = 4$]	$3.9_{-1.4}^{+2.2}$ ms [$\ell = 4$]	$3.2_{-1.1}^{+1.8}$ ms [$\ell = 4$]	[44]
(110, 279)	9.84 ± 0.06	$0.20_{-0.04}^{+0.05}$ s	$0.15_{-0.05}^{+0.07}$ s	$0.17_{-0.05}^{+0.08}$ s	$0.13_{-0.04}^{+0.06}$ s	[40]
(109, 276)	9.85 ± 0.06	$0.72_{-0.25}^{+0.97}$ s	$0.37_{-0.12}^{+0.17}$ s [$\ell = 4$]	$0.41_{-0.13}^{+0.19}$ s [$\ell = 4$]	$0.33_{-0.10}^{+0.16}$ s [$\ell = 4$]	[42, 43]
(109, 275)	10.48 ± 0.09	$9.7_{-4.4}^{+46}$ ms	$8.7_{-3.5}^{+5.9}$ ms [$\ell = 4$]	$9.4_{-3.8}^{+6.6}$ ms [$\ell = 4$]	$7.9_{-3.2}^{+5.4}$ ms [$\ell = 4$]	[42, 43]
(109, 274)	9.95 ± 0.10	440_{-170}^{+810} ms	220_{-99}^{+195} ms [$\ell = 4$]	242_{-112}^{+211} ms [$\ell = 4$]	200_{-94}^{+170} ms [$\ell = 4$]	[44]
(108, 275)	9.44 ± 0.06	$0.19_{-0.07}^{+0.22}$ s	$0.46_{-0.15}^{+0.23}$ s	$0.51_{-0.17}^{+0.25}$ s	$0.42_{-0.14}^{+0.21}$ s	[40]
(107, 272)	9.15 ± 0.06	$9.8_{-3.5}^{+11.7}$ s	$9.0_{-3.1}^{+4.7}$ s [$\ell = 4$]	$9.7_{-3.3}^{+5.1}$ s [$\ell = 4$]	$7.9_{-2.7}^{+4.1}$ s [$\ell = 4$]	[42, 43]
(107, 270)	9.11 ± 0.08	61_{-28}^{+292} s	73_{-30}^{+58} s [$\ell = 6$]	84_{-36}^{+64} s [$\ell = 6$]	70_{-30}^{+54} s [$\ell = 6$]	[44]
(106, 271)	8.67 ± 0.08	$1.9_{-0.6}^{+2.4}$ min	$2.10_{-0.95}^{+1.77}$ min [$\ell = 4$]	$2.27_{-1.02}^{+1.99}$ min [$\ell = 4$]	$1.83_{-0.83}^{+1.54}$ min [$\ell = 4$]	[40]
RMSD	-	-	0.209	0.198	0.218	

The heavy nuclei under study in the present work are neutron-rich but are located on the neutron-deficient side of beta-stability. Thus, β decay does not occur for these nuclei. Table IV shows our results on the observed α decay half-lives of heavy nuclei. Our results are obtained with the three models for nuclear density profiles and are compared with experimental data. The theoretical uncertainties shown in the table come from those of the experimental Q values. The obtained half-lives depend on the relative orbital angular momentum ℓ . We assume $\ell = 0$ for even-even decay cases but we allow the variation of ℓ in other types of decay processes. The value of ℓ which minimizes the difference with the experimental data for the half-life is explicitly shown in Table IV. The results for half-lives without the value of ℓ are obtained with $\ell = 0$. Compared with the previous results given in Ref. [21] which used a simple Fermi density profile, using realistic proton distribution improves the rms deviation (RMSD) in α decay lifetimes as shown in the table, which

is defined by

$$\text{RMSD} = \sqrt{\frac{1}{N-1} \sum_i \left(\log_{10} \left[\frac{T_i^{\text{expt.}}}{T_i^{\text{cal.}}} \right] \right)^2}, \quad (22)$$

where N is the total number of data. This indicates that the density profile of the neutron-rich heavy nuclei deviates from the simple Fermi density profile and its effect should be considered to get more realistic results.

Presented in Table V are our predictions on the half-lives of unobserved α decays of superheavy elements. In this case, the Q values are estimated by using the LDM and the local formula as described in Sec. II. We assume $\ell = 0$ for simplicity as there is no information on these processes.² Note that the half-lives from the D1S calculation are longer than the ones from SLy4 and DD-ME2

² If $\ell \neq 0$, the potential barrier width becomes larger than the case of $\ell = 0$ and the lifetime becomes longer. For example, when $Q = 11 \sim 14$ MeV, if we use the Gogny D1S model, the

calculations. We found that this is mostly caused by the differences in parameters given in Table III.

Figure 2 shows one of the most important α decay chains of superheavy nuclei, namely, the decay chains of $^{294}_{118}\text{Og}$ and $^{296}_{118}\text{Og}$. Our results successfully explain the α decay lifetimes in these two decay channels compared with experimental results. The α decay of $^{296}_{118}\text{Og}$ is yet to be discovered and the half-lives for this decay given in Fig. 2 are our predictions. It should be noticed that the half-lives shown in Fig. 2 are calculated from the nuclear α decay but the actual half-lives should be determined through the competition with the spontaneous fission process. For example, in the case of ^{286}Fl , although the measured half-life is $T^{\text{Exp.}} \approx 0.13$ s, the branching ratio of the α -decay is about 60% [45, 46], which makes the α -decay half-life close to 0.22 s.

Figure 3 shows the α potentials, $V_N + V_C$, used to calculate the half-life of $^{296}_{118}\text{Og}$ in this work. The dotted line indicates the Q -values obtained in this work. The double folding potential is presented by the dashed line for comparison [47]. This shows that, although the details of the potentials in each model are quite different inside the nucleus, the barrier widths corresponding to the obtained Q values are relatively close to each other. The slightly lower barrier in Ref. [47] is compensated by a preformation factor of 0.09, finally leading to half-lives close to each other.

V. SUMMARY AND CONCLUSION

In this paper, we have investigated the nuclear α decays of heavy nuclei based on nuclear energy density functional. We use a Skyrme-type force model to get the nuclear potential of the α particle inside a nucleus as a functional of proton and neutron density profiles of the daughter nucleus. These nucleon density profiles are obtained from the Skyrme SLy4, Gogny D1S, and relativistic mean-field DD-ME2 models. The parameters of the

nuclear potential of the α are fitted for each density profile model to measured α decay half-lives of heavy nuclei. The results show that this approach improves the previous results reported in Ref. [21], by reducing the RMS deviation from 0.238 to 0.198 \sim 0.218. In particular, we found that the Gogny D1S gives a better description among the models considered in the present work.

Once all the parameters are fixed, we apply the model to predict half-lives of unobserved α decays to get the estimations shown in Table V. One interesting quantity is the half-life of $^{296}_{118}\text{Og}$ as there are attempts to synthesize this nuclide [48]. Our predictions on this decay are also shown in Fig. 2, which shows our estimation of the Q value as $Q^{\text{LDM}} = 11.66$ MeV and $Q^{\text{Local}} = 11.47$ MeV. Our predictions on the half-life of the α decay of this nuclide is in the range of 0.86 ms \sim 3.48 ms, which is in good agreement with the predictions of Ref. [48] that gives 0.5 ms \sim 4.8 ms based on realistic mass formulas and with the prediction of Ref. [47] which obtained 0.825 ms using the double-folding potential model. (See also Refs. [49, 50].)

In the present work, we assumed that the potential for the α is isotropic. However, in the case of heavy nuclei, the deformation effects should be included, in particular, to understand its fine structure [51, 52]. Therefore, improving the present model by including deformation and other microscopic effects would be desired for a better understanding of nuclear α decays of superheavy nuclei.

ACKNOWLEDGMENTS

We are grateful to P. Papakonstantinou for providing us with density profiles of nuclei obtained in the Gogny force model. We also thank P. Mohr for providing his double folding potential for α decay and many suggestions for this work. The work of Y.O. was supported by Kyungpook National University Bokhyeon Research Fund, 2015.

-
- [1] P. Möller, The limits of the nuclear chart set by fission and alpha decay, EPJ Web Conf. **131**, 03002 (2016).
- [2] A. Gade and B. M. Sherrill, NSCL and FRIB at Michigan State University: Nuclear science at the limits of stability, Phys. Scripta **91**, 053003 (2016).
- [3] J. Gerl, M. Górska, and H. J. Wollersheim, Towards detailed knowledge of atomic nuclei — the past, present and future of nuclear structure investigations at GSI, Phys. Scripta **91**, 103001 (2016).
- [4] H. Grawe, K. Langanke, and G. Martínez-Pinedo, Nuclear structure and astrophysics, Rep. Prog. Phys. **70**, 1525 (2007).
- [5] Yu. Ts. Oganessian, A. Sobczewski, and G. M. Ter-Akopian, Superheavy nuclei: from predictions to discovery, Phys. Scripta **92**, 023003 (2017).
- [6] V. E. Viola, Jr. and G. T. Seaborg, Nuclear systematics of the heavy elements - II. Lifetimes for alpha, beta and spontaneous fission decay, J. Inorg. Nucl. Chem. **28**, 741 (1966).
- [7] G. Audi, M. Wang, A. H. Wapstra, F. G. Kondev, M. MacCormick, X. Xu, and B. Pfeiffer, The AME2012 atomic mass evaluation (I). Evaluation of input data, adjustment procedures, Chin. Phys. C **36**, 1287 (2012).
- [8] M. Wang, G. Audi, A. H. Wapstra, F. G. Kondev, M. MacCormick, X. Xu, and B. Pfeiffer, The AME2012 atomic mass evaluation (II). Tables, graphs and references, Chin. Phys. C **36**, 1603 (2012).

enhancement factors for the half-life become 1.06, 1.61, 2.16, 4.40, and 8.08 as we increase the value of ℓ from 1 to 5. Other models give similar results.

TABLE V. Predictions on the α decay lifetimes for unobserved superheavy elements with Q values from the LDM (case II) and from the local formula.

Nuclei (Z, A)	Q (MeV)				Q (MeV)			
	LDM	$T_{1/2}^{\text{SLy4}}$ (s)	$T_{1/2}^{\text{D1S}}$ (s)	$T_{1/2}^{\text{DD-ME2}}$ (s)	Local formula	$T_{1/2}^{\text{SLy4}}$ (s)	$T_{1/2}^{\text{D1S}}$ (s)	$T_{1/2}^{\text{DD-ME2}}$ (s)
(122, 307)	12.594	9.467×10^{-5}	9.982×10^{-5}	6.999×10^{-5}	12.289	4.340×10^{-4}	4.514×10^{-4}	3.194×10^{-4}
(122, 306)	12.729	5.649×10^{-5}	5.836×10^{-5}	4.183×10^{-5}	12.420	2.517×10^{-4}	2.688×10^{-4}	1.891×10^{-4}
(122, 305)	12.853	3.334×10^{-5}	3.607×10^{-5}	2.525×10^{-5}	12.550	1.402×10^{-4}	1.539×10^{-4}	1.073×10^{-4}
(122, 304)	12.986	1.931×10^{-5}	2.100×10^{-5}	1.480×10^{-5}	12.679	7.919×10^{-5}	8.911×10^{-5}	6.193×10^{-5}
(122, 303)	13.108	1.145×10^{-5}	1.300×10^{-5}	9.047×10^{-6}	12.807	4.646×10^{-5}	5.237×10^{-5}	3.593×10^{-5}
(122, 302)	13.239	6.692×10^{-6}	7.539×10^{-6}	5.339×10^{-6}	12.935	2.646×10^{-5}	3.000×10^{-5}	2.099×10^{-5}
(121, 306)	12.114	5.360×10^{-4}	5.522×10^{-4}	3.846×10^{-4}	11.853	2.104×10^{-3}	2.175×10^{-3}	1.509×10^{-3}
(121, 305)	12.250	2.948×10^{-4}	3.093×10^{-4}	2.170×10^{-4}	11.985	1.143×10^{-3}	1.212×10^{-3}	8.467×10^{-4}
(121, 304)	12.367	1.664×10^{-4}	1.831×10^{-4}	1.274×10^{-4}	12.117	6.082×10^{-4}	6.787×10^{-4}	4.700×10^{-4}
(121, 303)	12.511	9.077×10^{-5}	1.030×10^{-4}	7.119×10^{-5}	12.248	3.317×10^{-4}	3.794×10^{-4}	2.593×10^{-4}
(121, 302)	12.636	5.323×10^{-5}	6.026×10^{-5}	4.191×10^{-5}	12.378	1.834×10^{-4}	2.093×10^{-4}	1.439×10^{-4}
(121, 301)	12.769	2.976×10^{-5}	3.401×10^{-5}	2.378×10^{-5}	12.508	1.027×10^{-4}	1.169×10^{-4}	8.201×10^{-5}
(120, 304)	11.790	1.567×10^{-3}	1.650×10^{-3}	1.167×10^{-3}	11.546	5.792×10^{-3}	6.146×10^{-3}	4.349×10^{-3}
(120, 303)	11.918	8.584×10^{-4}	9.358×10^{-4}	6.494×10^{-4}	11.679	2.987×10^{-3}	3.331×10^{-3}	2.289×10^{-3}
(120, 302)	12.055	4.456×10^{-4}	5.025×10^{-4}	3.459×10^{-4}	11.812	1.561×10^{-3}	1.761×10^{-3}	1.217×10^{-3}
(120, 301)	12.181	2.491×10^{-4}	2.816×10^{-4}	1.959×10^{-4}	11.944	8.288×10^{-4}	9.395×10^{-4}	6.575×10^{-4}
(120, 300)	12.317	1.342×10^{-4}	1.523×10^{-4}	1.068×10^{-4}	12.076	4.465×10^{-4}	5.053×10^{-4}	3.520×10^{-4}
(120, 299)	12.442	7.735×10^{-5}	8.978×10^{-5}	6.175×10^{-5}	12.207	2.436×10^{-4}	2.817×10^{-4}	1.957×10^{-4}
(119, 298)	11.973	4.022×10^{-4}	4.688×10^{-4}	3.243×10^{-4}	11.772	1.131×10^{-3}	1.322×10^{-3}	8.986×10^{-4}
(119, 297)	12.109	2.119×10^{-4}	2.415×10^{-4}	1.706×10^{-4}	11.904	5.932×10^{-4}	1.610×10^{-3}	4.795×10^{-4}
(119, 296)	12.234	1.181×10^{-4}	1.340×10^{-4}	9.719×10^{-5}	12.036	3.147×10^{-4}	3.587×10^{-4}	2.593×10^{-4}
(119, 295)	12.368	6.172×10^{-5}	7.814×10^{-5}	5.316×10^{-5}	12.167	1.643×10^{-4}	1.913×10^{-4}	1.405×10^{-4}
(119, 294)	12.492	3.425×10^{-5}	4.112×10^{-5}	2.983×10^{-5}	12.297	8.668×10^{-5}	1.044×10^{-4}	7.549×10^{-5}
(119, 293)	12.625	1.874×10^{-5}	2.264×10^{-5}	1.646×10^{-5}	12.427	4.775×10^{-5}	5.767×10^{-5}	4.168×10^{-5}
(118, 298)	11.393	4.077×10^{-3}	4.600×10^{-3}	3.215×10^{-3}	11.197	1.206×10^{-2}	1.373×10^{-2}	9.535×10^{-3}
(118, 297)	11.522	2.126×10^{-3}	2.488×10^{-3}	1.699×10^{-3}	11.332	5.977×10^{-3}	7.008×10^{-3}	4.774×10^{-3}
(118, 296)	11.660	1.068×10^{-3}	1.238×10^{-3}	8.599×10^{-4}	11.466	3.013×10^{-3}	3.481×10^{-3}	2.423×10^{-3}
(118, 295)	11.787	5.640×10^{-4}	6.577×10^{-4}	4.692×10^{-4}	11.600	1.500×10^{-3}	1.762×10^{-3}	1.244×10^{-3}
(118, 294)	11.924	2.824×10^{-4}	8.069×10^{-4}	2.412×10^{-4}	11.733	7.515×10^{-4}	9.050×10^{-4}	6.387×10^{-4}
(118, 293)	12.050	1.516×10^{-4}	1.835×10^{-4}	1.305×10^{-4}	11.865	3.832×10^{-4}	4.644×10^{-4}	3.289×10^{-4}
(117, 298)	10.779	6.202×10^{-2}	7.032×10^{-2}	4.795×10^{-2}	10.920	1.678×10^{-1}	1.916×10^{-1}	1.311×10^{-1}
(117, 297)	10.920	2.837×10^{-2}	3.274×10^{-2}	2.236×10^{-2}	10.749	7.769×10^{-2}	9.001×10^{-2}	6.129×10^{-2}
(117, 296)	11.051	1.409×10^{-2}	1.666×10^{-2}	1.126×10^{-2}	10.886	3.620×10^{-2}	4.330×10^{-2}	2.903×10^{-2}
(117, 295)	11.192	6.660×10^{-3}	7.806×10^{-3}	5.400×10^{-3}	11.023	1.735×10^{-2}	2.035×10^{-2}	1.396×10^{-2}
(117, 294)	11.321	3.310×10^{-3}	3.965×10^{-3}	6.634×10^{-3}	11.158	8.146×10^{-3}	9.736×10^{-3}	6.779×10^{-3}
(117, 293)	11.460	1.584×10^{-3}	1.941×10^{-3}	1.325×10^{-3}	11.293	3.885×10^{-3}	4.752×10^{-3}	3.244×10^{-3}

- [9] H. J. Mang, Alpha decay, *Ann. Rev. Nucl. Sci.* **14**, 1 (1964).
- [10] Y. Oganessian, Heaviest nuclei from ^{48}Ca -induced reactions, *J. Phys. G* **34**, R165 (2007).
- [11] K. Morita *et al.*, New result in the production and decay of an isotope, $^{278}113$, of the 113th element, *J. Phys. Soc. Japan* **81**, 103201 (2012).
- [12] J. Khuyagbaatar *et al.*, $^{48}\text{Ca} + ^{249}\text{Bk}$ fusion reaction leading to element $Z = 117$: Long-lived α -decaying ^{270}Db and discovery of ^{266}Lr , *Phys. Rev. Lett.* **112**, 172501 (2014).
- [13] B. Buck, A. C. Merchant, and S. M. Perez, Ground state to ground state alpha decays of heavy even-even nuclei, *J. Phys. G* **17**, 1223 (1991).
- [14] B. Buck, A. C. Merchant, and S. M. Perez, Favoured alpha decays of odd-mass nuclei, *J. Phys. G* **18**, 143 (1992).
- [15] B. Buck, A. C. Merchant, and S. M. Perez, α decay calculations with a realistic potential, *Phys. Rev. C* **45**, 2247 (1992).
- [16] J. Dong, W. Zuo, J. Gu, Y. Wang, and B. Peng, α -decay half-lives and Q_α values of superheavy nuclei, *Phys. Rev. C* **81**, 064309 (2010).

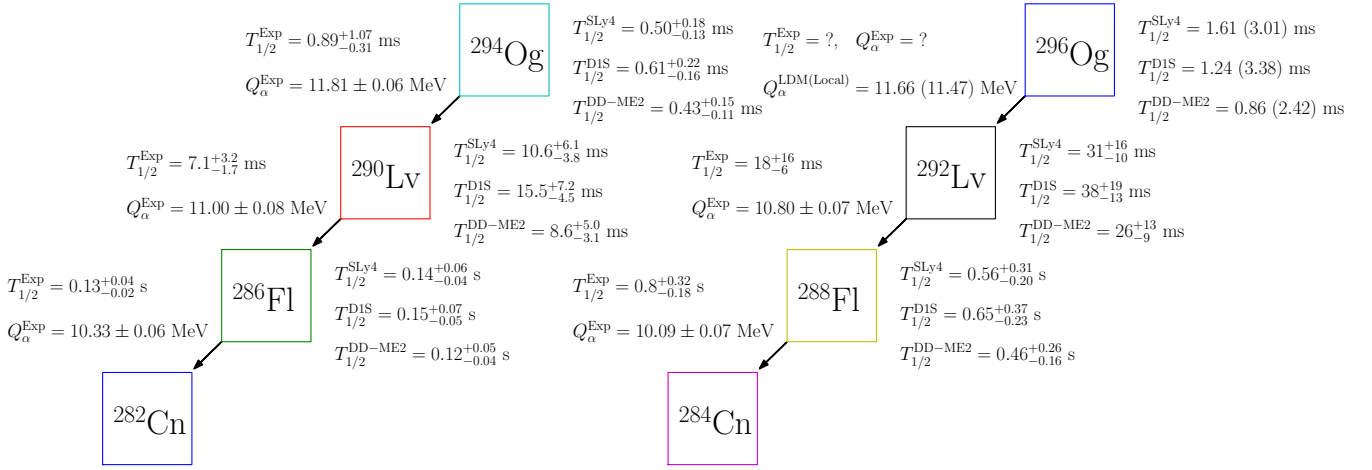


FIG. 2. Float charts for α decay chains for $^{294}_{118}\text{Og}$ and $^{296}_{118}\text{Og}$. The measured half-life of $^{286}_{118}\text{Fl}$ is about 0.13 s. Since the branching ratio of its α decay is about 60% [45, 46], however, the half-life of its α decay is about 0.22 s.

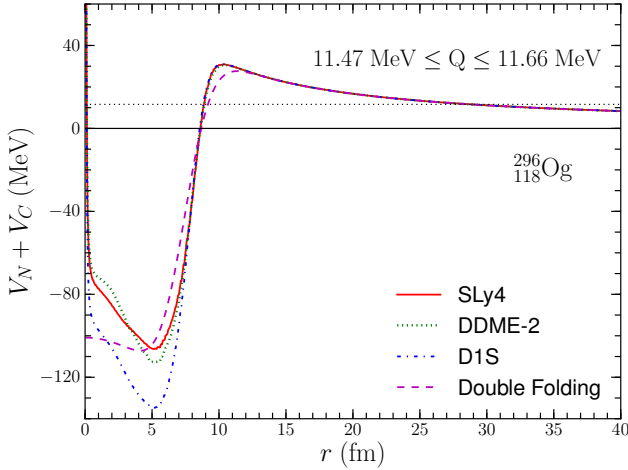


FIG. 3. The α nuclear and Coulomb potentials, $V_N + V_C$, for $^{296}_{118}\text{Og}$ in the models of the present work. The double folding potential for $^{296}_{118}\text{Og}$ of Ref. [47] is also presented for comparison.

[17] P. Roy Chowdhury, C. Samanta, and D. N. Basu, α decay half-lives of new superheavy elements, *Phys. Rev. C* **73**, 014612 (2006).
 [18] C. Samanta, P. R. Chowdhury, and D. N. Basu, Predictions of alpha decay half lives of heavy and superheavy elements, *Nucl. Phys. A* **789**, 142 (2007).
 [19] P. Roy Chowdhury, C. Samanta, and D. N. Basu, Search for long lived heaviest nuclei beyond the valley of stability, *Phys. Rev. C* **77**, 044603 (2008).
 [20] H. Geiger and J. M. Nuttall, The ranges of the α particles from various substances and a relation between range and period of transformation, *Phil. Mag. Ser. 6* **22**, 613 (1911).
 [21] E. Shin, Y. Lim, C. H. Hyun, and Y. Oh, Nuclear isospin asymmetry and α decay of heavy nuclei, *Phys. Rev. C* **94**, 024320 (2016).

[22] E. Chabanat, P. Bonche, P. Haensel, J. Meyer, and R. Schaeffer, A Skyrme parametrization from subnuclear to neutron star densities Part II. Nuclei far from stabilities, *Nucl. Phys. A* **635**, 231 (1998), **643**, 441(E) (1998).
 [23] J. F. Berger, M. Girod, and D. Gogny, Time-dependent quantum collective dynamics applied to nuclear fission, *Computer Phys. Comm.* **63**, 365 (1991).
 [24] G. A. Lalazissis, T. Nikšić, D. Vretenar, and P. Ring, New relativistic mean-field interaction with density-dependent meson-nucleon couplings, *Phys. Rev. C* **71**, 024312 (2005).
 [25] A. W. Steiner, M. Prakash, J. M. Lattimer, and P. J. Ellis, Isospin asymmetry in nuclei and neutron stars, *Phys. Rep.* **411**, 325 (2005).
 [26] W. D. Myers and W. J. Swiatecki, Average nuclear properties, *Ann. Phys. (N.Y.)* **55**, 395 (1969).
 [27] A. Tamii *et al.*, Complete electric dipole response and the neutron skin in ^{208}Pb , *Phys. Rev. Lett.* **107**, 062502 (2011).
 [28] PREX Collaboration, S. Abrahamyan *et al.*, Measurement of the neutron radius of ^{208}Pb through parity violation in electron scattering, *Phys. Rev. Lett.* **108**, 112502 (2012).
 [29] C. J. Horowitz *et al.*, Weak charge form factor and radius of ^{208}Pb through parity violation in electron scattering, *Phys. Rev. C* **85**, 032501(R) (2012).
 [30] Crystal Ball at MAMI and A2 Collaboration, C. M. Tarbert *et al.*, Neutron skin of ^{208}Pb from coherent pion photoproduction, *Phys. Rev. Lett.* **112**, 242502 (2014).
 [31] D. G. Ravenhall, C. J. Pethick, and J. M. Lattimer, Nuclear interface energy at finite temperatures, *Nucl. Phys. A* **407**, 571 (1983).
 [32] Y. Lim, *Theory of nuclear matter of neutron stars and core collapsing supernovae*, PhD thesis, Stony Brook University, 2012.
 [33] J. Duflo and A. P. Zuker, Microscopic mass formulas, *Phys. Rev. C* **52**, R23 (1995).
 [34] A. E. L. Dieperink and P. Van Isacker, Shell corrections to a liquid-drop description of nuclear masses and radii,

- Eur. Phys. J. A **42**, 269 (2009).
- [35] E. L. Medeiros, M. M. N. Rodrigues, S. B. Duarte, and O. A. P. Tavares, Systematics of alpha-decay half-life: New evaluations for alpha-emitter nuclides, J. Phys. G **32**, B23 (2006).
- [36] T. Dong and Z. Ren, Improved version of a binding energy formula for heavy and superheavy nuclei with $Z \geq 90$ and $N \geq 140$, Phys. Rev. C **77**, 064310 (2008).
- [37] R. E. Langer, On the connection formulas and the solutions of the wave equation, Phys. Rev. **51**, 669 (1937).
- [38] J. Decharge and D. Gogny, Hartree-Fock-Bogolyubov calculations with the $D1$ effective interactions on spherical nuclei, Phys. Rev. C **21**, 1568 (1980).
- [39] T. Nikšić, N. Paar, D. Vretenar, and P. Ring, DIRHB – A relativistic self-consistent mean-field framework for atomic nuclei, Comput. Phys. Commun. **185**, 1808 (2014).
- [40] Yu. Ts. Oganessian *et al.*, Synthesis of the isotopes of elements 118 and 116 in the ^{249}Cf and $^{249}\text{Cm} + ^{48}\text{Ca}$ fusion reactions, Phys. Rev. C **74**, 044602 (2006).
- [41] Yu. Ts. Oganessian *et al.*, Measurements of cross sections and decay properties of the isotopes of elements 112, 114, and 116 produced in the fusion reactions $^{233,238}\text{U}$, ^{242}Pu , and $^{248}\text{Cm} + ^{48}\text{Ca}$, Phys. Rev. C **70**, 064609 (2004), **71**, 029902(E) (2005).
- [42] Yu. Ts. Oganessian *et al.*, Experiments on the synthesis of element 115 in the reaction $^{243}\text{Am}(^{48}\text{Ca}, xn)^{291-x}115$, Phys. Rev. C **69**, 021601(R) (2004), **69**, 029902(E) (2004).
- [43] Yu. Ts. Oganessian *et al.*, Synthesis of elements 115 and 113 in the reaction $^{243}\text{Am} + ^{48}\text{Ca}$, Phys. Rev. C **72**, 034611 (2005).
- [44] Yu. Ts. Oganessian *et al.*, Synthesis of the isotope $^{282}113$ in the $^{237}\text{Np} + ^{48}\text{Ca}$ fusion reaction, Phys. Rev. C **76**, 011601(R) (2007).
- [45] Yu. Ts. Oganessian and V. K. Utyonkov, Super-heavy element research, Rep. Prog. Phys. **78**, 036301 (2015).
- [46] Yu. Ts. Oganessian and V. K. Utyonkov, Superheavy nuclei from ^{48}Ca -induced reactions, Nucl. Phys. A **944**, 62 (2015).
- [47] P. Mohr, α -decay properties of $^{296}118$ from double-folding potentials, Phys. Rev. C **95**, 011302(R) (2017).
- [48] A. Sobiczewski, Theoretical predictions for the nucleus $^{296}118$, Phys. Rev. C **94**, 051302(R) (2016).
- [49] K. P. Santhosh, B. Priyanka, and C. Nithya, Feasibility of observing the α decay chains from isotopes of SHN with $Z = 128$, $Z = 126$, $Z = 124$ and $Z = 122$, Nucl. Phys. A **955**, 156 (2016).
- [50] H. C. Manjunatha, Theoretical prediction of probable isotopes of superheavy nuclei of $Z = 122$, Int. J. Mod. Phys. E **25**, 1650100 (2016).
- [51] D. S. Delion, A. Insolia, and R. J. Liotta, Anisotropy in alpha decay of odd-mass deformed nuclei, Phys. Rev. C **46**, 884 (1992).
- [52] D. Ni and Z. Ren, New approach for α -decay calculations of deformed nuclei, Phys. Rev. C **81**, 064318 (2010).